An electrically tunable metasurface integrated with graphene for mid-infrared light modulation*

Zongpeng Wang(王宗鹏)[1], Ya Deng(邓娅)[2], and LianFeng Sun(孙连峰)[2,†]

[1] State Key Laboratory for Mesoscopic Physics, School of Physics, Peking University, Beijing 100871, China
[2] National Center for Nanoscience and Technology, Beijing 100871, China

(Received 5 May 2017; revised manuscript received 22 June 2017; published online 30 September 2017)

We propose a low-cost plasmonic metasurface integrated with single-layer graphene for dynamic modulation of mid-infrared light. The plasmonic metasurface is composed of an array of split magnetic resonators (MRs) where a nano slit is included. Extraordinary optical transmission (EOT) through the deep subwavelength slit is observed by excitation of magnetic plasmons in the split MRs. Furthermore, the introduction of the slit provides strongly enhanced fields around the graphene layer, leading to a large tuning effect on the EOT by changing the Fermi energy of the graphene. The proposed metasurface can be utilized as an optical modulator with a broad modulation width (15 μm) or an optical switch with a high on/off ratio (>100). Meanwhile, the overall thickness of the metasurface is 430 nm, which is tens of times smaller than the operating wavelength. This work may have potential applications in mid-infrared optoelectrical devices and give insights into reconfigurable flat optics and optoelectronics.

Keywords: metasurface, graphene, optical modulator, magnetic plasmon

PACS: 41.20.Jb, 42.25.Bs, 81.05.ue **DOI:** 10.1088/1674-1056/26/11/114101

1. Introduction

Metasurfaces, which are composed of artificially arranged plasmonic resonators, are the two-dimensional (2D) counterpart of metamaterials with deep subwavelength thicknesses.[1–3] The development of metasurfaces has opened up possibilities to manipulate electromagnetic (EM) waves in an unprecedented manner. For example, a series of phase-gradient metasurfaces have been proposed to introduce abrupt phase changes to the incident light at nanoscale, thus to modulate the propagation of light beyond the law of reflection and refraction.[4–9] Other potential applications of metasurfaces include optical vertex,[10,11] holograms,[12–15] and nonlinear optics,[16–19] to name just a few. Although considerable progress has been made, the application of metasurfaces still faces a major challenge. That is the lack of dynamic tunability once the metasurface is fabricated.[20] Various approaches have been developed to dynamically tune the optical response of plasmonic resonators, including thermal,[21,22] mechanical,[23,24] and optical[25] mechanisms. However, those methods are not favorable in terms of response time and Si technology compatibility.

Graphene, the first member in the 2D material family, has drawn tremendous attention over the last decade due to its unique electronic and optical properties,[26,27] with promising applications in a wide range of fields.[28–33] Specifically, the Dirac point in the graphene band structure enables a large field effect, which thus can be exploited to tune the optical property of graphene through a simple Si-technology-compatible gate voltage.[26] Furthermore, with a carrier mobility exceeding 200000 $cm^2 \cdot V^{-1} \cdot s^{-1}$ at room temperature in graphene, electrical devices based on graphene are expected to operate at extremely high speed.[32] Therefore, the large field effect, the high operation speed, and Si technology compatibility together make graphene an ideal platform for tuning the resonance of plasmonic structures after fabrication.[20] Metasurfaces based on graphene and plasmonic structures have been well demonstrated.[34–39] Several optical modulators formed by the combination of plasmonic structures and graphene have been proposed.[40–45] However, they are mostly based on the modulation of the reflected light and the modulation depth is relatively low. In practice, a modulator based on the modulation of the transmitted light with deep modulation depth is also desired.

In this paper, we propose a plasmonic metasurface integrated with graphene for dynamic modulation of the transmitted light at the mid-infrared regime. The plasmonic metasurface is composed of an array of split magnetic resonators (MRs), where a slit is introduced in the middle compared with the traditional MRs. The introduction of the slit provides electric field "hot areas" to enhance the interaction strength between graphene and the plasmonic resonator array. To form an optical modulator, extraordinary optical transmission (EOT) is first induced by excitation of magnetic plasmons (MPs) in the resonators, then the EOT phenomenon is tuned by changing the Fermi energy of graphene. The proposed modulator provides a modulation depth over 10000% and an overall thick-

*Project supported by the National Natural Science Foundation of China (Grant Nos. 11174062 and 51472057).
†Corresponding author. E-mail: slf@nanoctr.cn
© 2017 Chinese Physical Society and IOP Publishing Ltd

ness of 430 nm, which is tens of times smaller than the operating wavelength. This work may have potential applications in mid-infrared optoelectrical devices and give insights to reconfigurable flat optics and optoelectronics.

2. Design and modeling of the plasmonic metasurface

Figure 1 depicts schematically the idea of designing a metasurface for modulating the optical transmission using graphene. First, a nano-sandwich magnetic resonator (Fig. 1(a)) is used as in perfect absorption applications due to its ability of generating artificial permeability by exciting magnetic plasmons.[46–50] It works as follows. Zero reflection can be achieved when the impedance matching condition (IMC) is fulfilled, where the impedance of the metasurface ($\sqrt{\mu/\varepsilon}$) is equal to the impedance of the vacuum. Meanwhile, the transmission is cut off by the metal film. With zero reflection and zero transmission, perfect absorption is realized. In this work, however, we come up with the so called split magnetic resonator where a slit is introduced in the middle of the nano-sandwich resonator, as shown in Fig. 1(b). The slit comes with three main consequences. 1) The slit shall be small enough with no damage to the excitation of magnetic plasmons to maintain the IMC and cancel the reflection. 2) The introduction of the slit opens up a transmission channel for light to pass through. In other words, EOT is included in the metasurface. 3) According to the material perturbation theory (MPT), graphene should be placed in an area where the electric field is greatly enhanced to maximize the modulation effect.[42] The slit provides such an area. Finally, as shown in Fig. 1(c), graphene is introduced at the vicinity of the slit to form the modulator. The changes of the Fermi energy of graphene will lead to large modulation of the transmitted light.

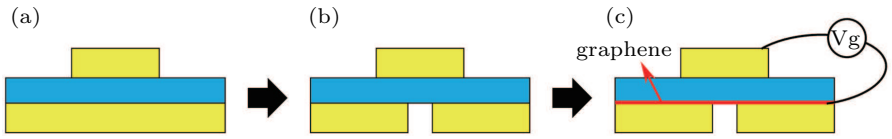


Fig. 1. (color online) Schematic illustration of the idea of designing a metasurface for modulating the optical transmission using graphene. The details are given in the text.

The three-dimensional (3D) schematic of the proposed structure is shown in Fig. 2. There are: a metal film with slits, a dielectric spacer, and a metal grating from bottom to top. The center of the grating is aligned to the center of the slits. The dashed rectangle in Fig. 2 marks the split MR. The geometric parameters are given as $L = 1.8$ μm, $P = 2.6$ μm, gap $= 40$ nm, $t_1 = t_3 = 40$ nm, and $t_2 = 350$ nm.

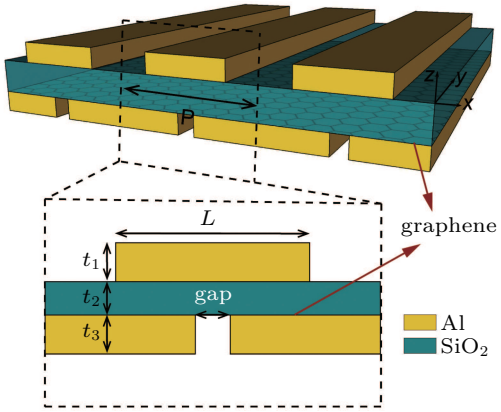


Fig. 2. (color online) Schematic of the proposed structure. The geometric parameters are $L = 1.8$ μm, $P = 2.6$ μm, gap $= 40$ nm, $t_1 = t_3 = 40$ nm, and $t_2 = 350$ nm.

We use the finite-difference time-domain (FDTD) method to simulate the optical response of the proposed metasurface. In the simulation, EM waves are incident along the z axis with the electric field polarized along the x axis. The periodic boundary condition is used in x and y directions and the perfect matched layer (PML) boundary condition is used in the z direction. All metals in the simulation are chosen to be Al to reduce the cost, with its permittivity extracted from experiment data.[51] The material of the dielectric spacer is set to be SiO_2 with a refractive index of 1.4. Graphene is modeled as an anisotropic ultrathin layer with a thickness of 0.33 nm. The in-plane permittivity of graphene is calculated as $\varepsilon_{\parallel} = \varepsilon_r + i\sigma/\varepsilon_0\omega\Delta$, where $\varepsilon_r = 2.5$ is the background permittivity, σ is the surface conductivity, and Δ is the thickness of the graphene. The out-of-plane permittivity is set to be $\varepsilon_{\perp} = \varepsilon_r = 2.5$. Here, σ is calculated under random-phase approximation (RPA) including contributions from both interband and intraband transitions, which is expressed as

$$\begin{aligned}\sigma(\omega) &= \frac{2e^2 k_B T}{\pi\hbar^2}\cdot\frac{i}{\omega + i\tau^{-1}}\log\left[2\cosh\left(\frac{E_F}{2k_B T}\right)\right] \\ &+ \frac{e^2}{4\hbar}\left(H(\omega/2) + i\frac{2\omega}{\pi}\int_0^{\infty}\frac{H(\omega'/2) - H(\omega/2)}{\omega^2 - \omega'^2}\,d\omega'\right), \quad (1)\end{aligned}$$

where $H(\omega) = \sinh(\hbar\omega/k_B T)/[\cosh(E_F/k_B T) + \cosh(\hbar\omega/k_B T)]$, $T = 300$ K is the temperature, E_F is the Fermi energy, and $\tau = \mu E_F/ev_F^2$ is the relaxation time, with the mobility $\mu = 10000$ cm^2/V·s and the Fermi velocity $v_F = 10^6$ m/s.

3. Results

The optical spectrum of the proposed metasurface is shown in Fig. 3 when the graphene Fermi energy is 0.4 eV. As

can be observed, a resonant phenomenon arises at ~ 15 μm. At resonance, the reflection approaches zero, indicating the introduction of a slit does not break the IMC as mentioned above. The transmission, however, reaches a high value of 68% due to the introduction of the slit. Note that the size of the slit is 40 nm, which is 1/375 of the resonant wavelength. Therefore, the proposed metasurface has the ability of sustaining a deep subwavelength EOT phenomenon. Increasing the size of the slit can further improve the transmission and reduce the absorption. However, the near field around the slit becomes weak if the slit is broadened, which is not favorable for graphene to take effect. To achieve both a high transmission and a large tuning effect, we choose the optimized slit size of 40 nm.

To understand the physical mechanism behind the resonance, we calculate the field distributions and show them in Fig. 4. The up panels are the electric fields while the down panels are the magnetic fields. Figures 4(b) and 4(d) are enlarged views around the slit and graphene, respectively. One can see that the electric field is strongly enhanced and localized in the slit. Furthermore, the electric field concentrates around the graphene layer, which means that the observed resonance can be largely tuned by changing the Fermi energy of graphene, as will be discussed below. We note that the graphene layer out of the slit region has little effect on the resonance, as the electric field outside the slit is rather weak. The magnetic field is also largely enhanced. In contrast with the electric field, the magnetic field is mainly distributed in the dielectric spacer circled by oppositely flowing currents, which indicates that MPs are excited in the sandwich split MR. After analysis of the field distributions, the underlying physics can be understood as follows. Incident EM waves excite MPs in the split MRs, which cancels the reflection by fulfilling the impedance matching condition. The EM waves then pass through the slits with the electric field strongly enhanced around graphene, providing an opportunity to dynamically tune the transmission by changing the optical property of graphene.

Figure 5(a) shows the transmission spectra of the proposed optical modulator with respect to different graphene Fermi energies. One can see that the transmission peaks are largely tuned by graphene. The transmission peak blue-shifts continuously with increasing Fermi energy and reaches a maximum at 0.4 eV. Specifically, the resonate peak locates at 27.5 μm when a low Fermi energy of 0.1 eV is applied. When a high Fermi energy of 0.9 eV is applied, the resonant peak

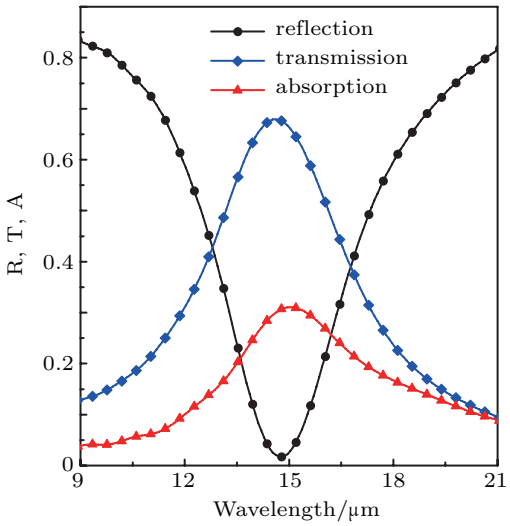


Fig. 3. (color online) Reflection, transmission, absorption spectra of the proposed metasurface.

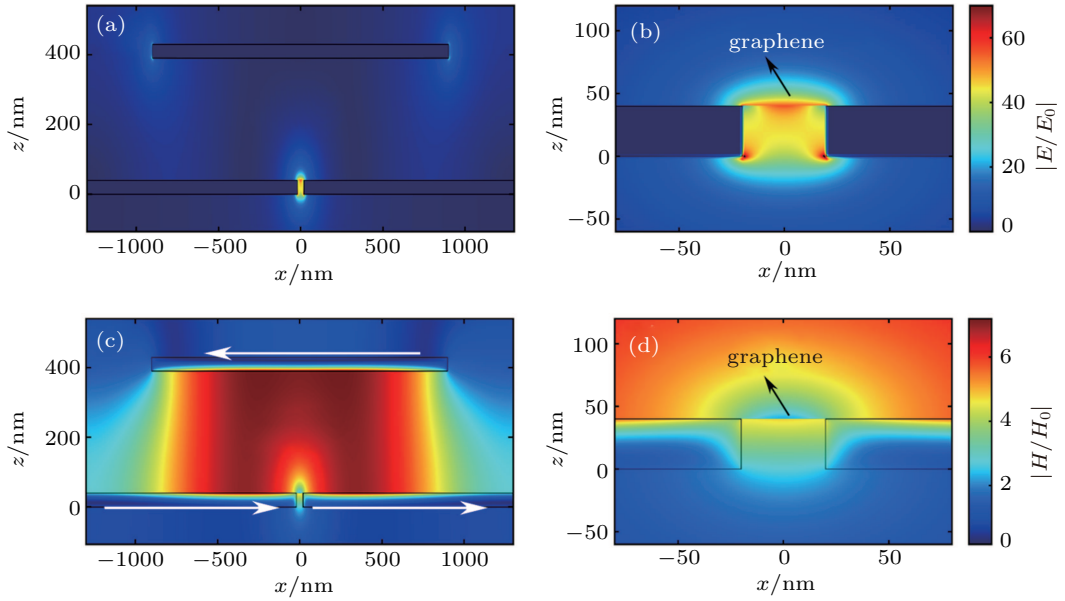


Fig. 4. (color online) (a) Electric field and (c) magnetic field distributions at resonance. Panels (b) and (d) are the enlarged views around the slit and graphene in panels (a) and (c), respectively. Black rectangles mark the areas where metal exists. The white arrows in panel (c) indicate schematically the current flow in the metals.

blue-shifts effectively to 10.5 μm, indicating a broad modulation width of 17 μm. Another key parameter to evaluate the performance of a modulator is the modulation depth. There are two common definitions of this parameter in earlier works: the absolute modulation depth (AMD) and the relative modulation depth (RMD). The absolute modulation depth at wavelength λ is defined as $\mathrm{AMD}^{\lambda} = T^{\lambda}_{\mathrm{Max}}(E_{\mathrm{F}}) - T^{\lambda}_{\mathrm{Min}}(E_{\mathrm{F}})$, while the relative modulation depth is defined as $\mathrm{RMD}^{\lambda} = \left[T^{\lambda}_{\mathrm{Max}}(E_{\mathrm{F}}) - T^{\lambda}_{\mathrm{Min}}(E_{\mathrm{F}})\right] / T^{\lambda}_{\mathrm{Min}}(E_{\mathrm{F}})$, where E_{F} is the Fermi energy, $T^{\lambda}_{\mathrm{Max}}(E_{\mathrm{F}})$ and $T^{\lambda}_{\mathrm{Min}}(E_{\mathrm{F}})$ are the maximum and the minimum of the transmission at wavelength λ as a function of E_{F}.

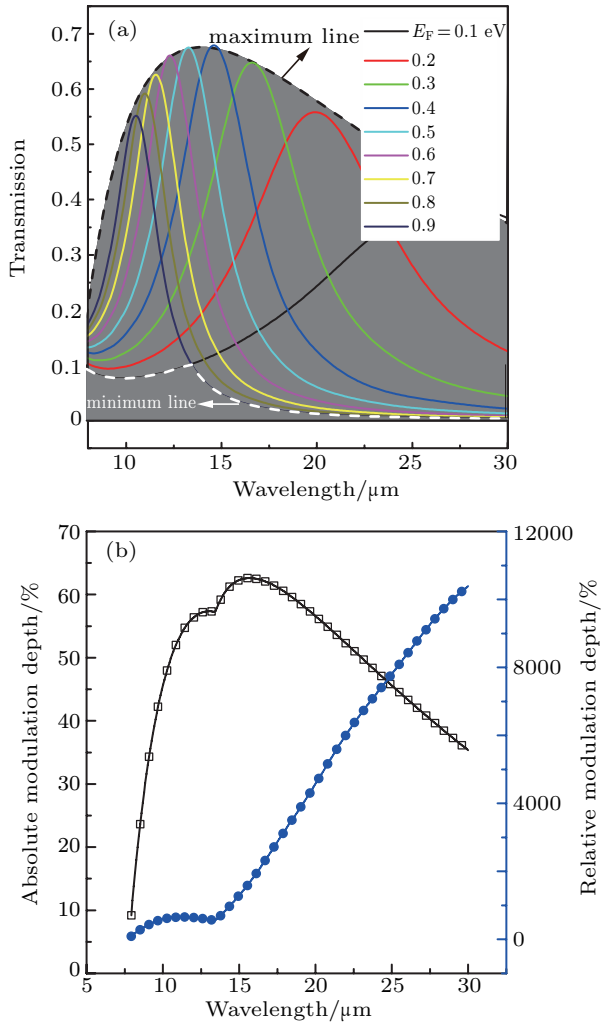


Fig. 5. (color online) (a) Modulation of mid-infrared light by changing the Fermi energy of graphene. The black and white dashed lines are the transmission maximum and minimum as a function of E_{F}, respectively. (b) The absolute modulation depth and relative modulation depth of the proposed modulator.

To examine the performance of the optical modulator proposed here, the transmission maximum and minimum at different E_{F} must be computed. The transmission minimum is easy to find, as the white dashed line shows in Fig. 5(a). The transmission maximum, however, is more complicated to define, because only finite numbers of simulations can be performed. To define the transmission maximum, we draw the envelope of the transmission peaks in Fig. 5(a), and use the envelope as the maximum line, as the black dashed line shows. The computed AMD and RMD are then shown in Fig. 5(b). The AMD first increases with longer wavelengths, reaches a peak at $\sim$ 15 μm, and then decreases after the peak. The max AMD of the proposed optical modulator is 63%, which is one of the best results among graphene-based plasmonic mid-infrared modulators. The RMD, however, mainly exhibits an increasing tendency with longer wavelengths. This is because the transmission minimum approaches zero at long wavelengths. The RMD exceeds 10000% at 30 μm, indicating that the modulator can also be used as an optical switch. In addition to the high on/off ratio, one can expect the proposed optical switch to operate at a fast speed up to 500 GHz,[31] considering the ultrahigh carrier mobility in graphene.

4. Discussion

In the above design of the plasmonic metasurface, the center of the metal grating bar and the center of the slit are supposed to be aligned, which is undesirable from an experimental point of view. In the next, we show that this alignment is not necessary. The case where the center of the grating bar and the center of the slit have an offset of Δ is schematically shown in Fig. 6(a). Two specific cases with Δ being 100 nm and 200 nm are considered. We note that experiment errors above 100 nm are easy to control within modern fabrication technology.

The corresponding transmission spectra are shown in Fig. 6(c). One can see that an offset as large as 200 nm hardly causes damage to the modulation effect. However, the overall transmission does drop a little and all the transmission peaks red-shift to longer wavelength with a larger offset. The negligible transmission drop with a relatively large structure change is due to the characteristic of the magnetic plasmon resonance. Magnetic plasmons can still be excited in the split MRs with an offset introduced. The red-shift behavior of the transmission peaks can be understood using an effective circuit model, which is shown in Fig. 6(b). In the circuit model, the metals behave like electrical inductance while the dielectric spacer and the slit gap behave like electrical capacitance. Graphene can be regarded as an additional impedance Z_{G}. For simplicity and not losing generality, Z_{G} is assumed to be zero in the analysis. The split MR then is modeled as an LC circuit with resonant wavelength $\lambda \propto \sqrt{LC}$, where L is the total inductance and C is the total capacitance. From the effective circuit, L and C can be calculated as $L = L_1 + 2L_2$ and $\mathrm{C} = (1/C_{\mathrm{s}} + 1/C_{\mathrm{m}})^{-1}$, where $1/C_{\mathrm{m}} = 1/C_1 + 1/C_2$. An offset does not affect the overlap area of the capacitor, therefore the sum of C_1 and C_2 is a constant. Obviously, it is when C_1 equals to C_2, the total C has a minimum. Thus, the metasurface has a shorter resonance wavelength when the split MR is aligned.

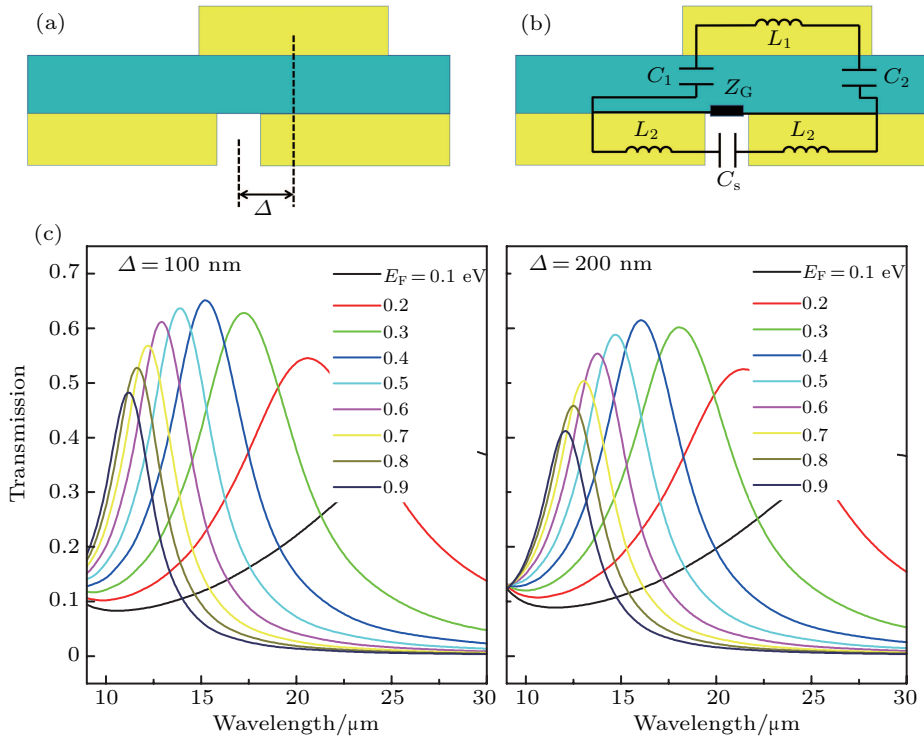


Fig. 6. (color online) (a) Schematic illustration of the split MR when an offset Δ is included. (b) The effective circuit of the structure. (c) Transmission spectra of two cases of $\Delta = 100$ nm and $\Delta = 200$ nm.

The possibility of fabrication is illustrated in Fig. 7. An Al film is first deposited on a Si substrate. Then the gaps are etched by focused ion beam (FIB). Next, a single layer of graphene is transferred, following the SiO_2 deposition process. Finally, the upmost grating is fabricated using electron beam lithography (EBL).

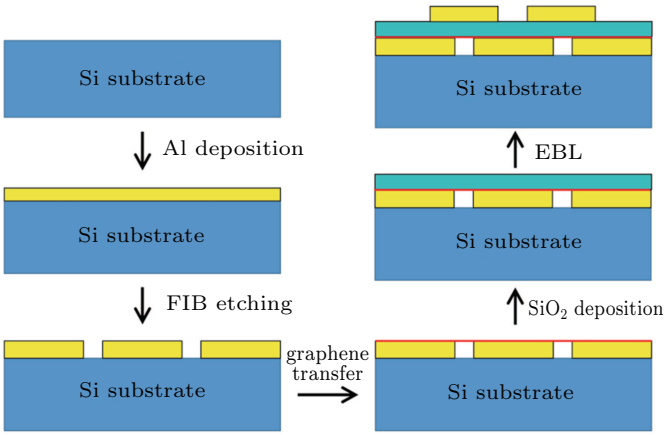


Fig. 7. (color online) Schematic illustration of the fabrication process.

5. Conclusion

In summary, we have integrated single-layer graphene with a plasmonic metasurface to achieve dynamic modulation for mid-infrared light. The proposed metasurface consists of an array of split MRs. Magnetic plasmons are excited in the split MR and take responsibility for the high transmission through the deep subwavelength slit. Strongly enhanced fields are formed in the slit and around the graphene, which ensures a large tuning effect of graphene. The proposed modulator has a modulation width of 15 μm and a modulation depth of over 10000%. Experimental error within 200 nm does not affect the modulation effect.

References

[1] Meinzer N, Barnes W L and Hooper I R 2014 *Nat. Photon.* **8** 889
[2] Yu N and Capasso F 2014 *Nat. Mater.* **13** 139
[3] Chen H T, Taylor A J and Yu N 2016 *Rep. Prog. Phys.* **79** 076401
[4] Yu N F, Genevet P, Kats M A, Aieta F, Tetienne J P, Capasso F and Gaburro Zet 2011 *Science* **334** 333
[5] Sun S, Yang K Y, Wang C M, Juan T K, Chen W T, Liao C Y, He Q, Xiao S, Kung W T and Guo G Y 2012 *Nano Lett.* **12** 6223
[6] Huang L, Chen X, Bai B, Tan Q, Jin G, Zentgraf T and Zhang S 2013 *Light-Sci. Appl.* **2** e70
[7] Pors A, Nielsen M G, Eriksen R L and Bozhevolnyi S I 2013 *Nano Lett.* **13** 829
[8] Li Y, Zhang J, Qu S, Wang J, Chen H, Xu Z and Zhang A 2014 *Appl. Phys. Lett.* **104** 221110
[9] Lin D, Fan P, Hasman E and Brongersma M L 2014 *Science* **345** 298
[10] Ma X, Pu M, Li X, Huang C, Wang Y, Pan W, Zhao B, Cui J, Wang C and Zhao Z 2015 *Sci. Rep.* **5** 10365
[11] Yang Y, Wang W, Moitra P, Kravchenko I I, Briggs D P and Valentine J 2014 *Nano Lett.* **14** 1394
[12] Huang L, Chen X, Mühlenbernd H, Zhang H, Chen S, Bai B, Tan Q, Jin G, Cheah K W and Qiu C W 2013 *Nat. Commun.* **4**
[13] Ni X, Kildishev A V and Shalaev V M 2013 *Nat. Commun.* **4**
[14] Wen D, Yue F, Li G, Zheng G, Chan K, Chen S, Chen M, Li K F, Wong P W H and Cheah K W 2015 *Nat. Commun.* **6**
[15] Zheng G, Mühlenbernd H, Kenney M, Li G, Zentgraf T and Zhang S 2015 *Nat. Nanotechnol.* **10** 308
[16] Chen P Y and Alù A 2010 *Phys. Rev. B* **82** 235405
[17] Lee J, Tymchenko M, Argyropoulos C, Chen P Y, Lu F, Demmerle F, Boehm G, Amann M C, Alu A and Belkin M A 2014 *Nature* **511** 65
[18] Li G, Chen S, Pholchai N, Reineke B, Wong P W H, Pun E Y B, Cheah K W, Zentgraf T and Zhang S 2015 *Nat. Mater.* **14** 607
[19] Minovich A E, Miroshnichenko A E, Bykov A Y, Murzina T V, Neshev D N and Kivshar Y S 2015 *Laser Photonics Rev.* **9** 195

[20] Emani N K, Kildishev A V, Shalaev V M and Boltasseva A 2015 *Nanophotonics* **4** 214

[21] Xu G, Huang C M, Tazawa M, Jin P and Chen D M 2008 *J. Appl. Phys.* **104** 053101

[22] Kats M A, Blanchard R, Genevet P, Yang Z, Qazilbash M M, Basov D, Ramanathan S and Capasso F 2013 *Opt. Lett.* **38** 368

[23] Chiang Y L, Chen C W, Wang C H, Hsieh C Y, Chen Y T, Shih H Y and Chen Y F 2010 *Appl. Phys. Lett.* **96** 041904

[24] Mahmoud M A 2015 *J. Phys. Chem. C* **119** 19359

[25] Abb M, Albella P, Aizpurua J and Muskens O L 2011 *Nano Lett.* **11** 2457

[26] Novoselov K S, Geim A K, Morozov S V, Jiang D, Zhang Y, Dubonos S V, Grigorieva I V and Firsov A A 2004 *Science* **306** 666

[27] Bonaccorso F, Sun Z, Hasan T and Ferrari A 2010 *Nat. Photon.* **4** 611

[28] Pang S, Hernandez Y, Feng X and Müllen K 2011 *Adv. Mater.* **23** 2779

[29] Liu M, Yin X, Ulin-Avila E, Geng B, Zentgraf T, Ju L, Wang F and Zhang X 2011 *Nature* **474** 64

[30] Liu M, Yin X and Zhang X 2012 *Nano Lett.* **12** 1482

[31] Xia F, Mueller T, Lin Y M, Valdes-Garcia A and Avouris P 2009 *Nat. Nanotechnol.* **4** 839

[32] Mueller T, Xia F and Avouris P 2010 *Nat. Photon.* **4** 297

[33] Fang Z, Liu Z, Wang Y, Ajayan P M, Nordlander P and Halas N J 2012 *Nano Lett.* **12** 3808

[34] Hu X and Wang J 2015 *Opt. Lett.* **40** 5538

[35] Hu X, Long Y, Ji M, Wang A, Zhu L, Ruan Z, Wang Y and Wang J 2016 *Opt. Express* **24** 7168

[36] Wang A, Hu X, Zhu L, Zeng M, Fu L and Wang J 2015 *Opt. Express* **23** 31728

[37] Hu X, Wang A, Zeng M, Long Y, Zhu L, Fu L and Wang J 2016 *Sci. Rep.* **6**

[38] Hu X and Wang J 2017 *IEEE Photonics J.* **9** 1

[39] Hu X and Wang J 2017 *IEEE J. Quantum Elect.* **53** 1

[40] Yu S, Wu X, Wang Y, Guo X and Tong L 2017 *Adv. Mater.*

[41] Yao Y, Kats M A, Genevet P, Yu N, Song Y, Kong J and Capasso F 2013 *Nano Lett.* **13** 1257

[42] Li Z and Yu N 2013 *Appl. Phys. Lett.* **102** 131108

[43] Yao Y, Kats M A, Shankar R, Song Y, Kong J, Loncar M and Capasso F 2013 *Nano Lett.* **14** 214

[44] Yao Y, Shankar R, Kats M A, Song Y, Kong J, Loncar M and Capasso F 2014 *Nano Lett.* **14** 6526

[45] Dabidian N, Kholmanov I, Khanikaev A B, Tatar K, Trendafilov S, Mousavi S H, Magnuson C, Ruoff R S and Shvets G 2015 *ACS Photon.* **2** 216

[46] Liu N, Mesch M, Weiss T, Hentschel M and Giessen H 2010 *Nano Lett.* **10** 2342

[47] Wang J and Du J 2016 *Appl. Sci.* **6** 239

[48] Hu C, Zhao Z, Chen X and Luo X 2009 *Opt. Express* **17** 11039

[49] Dang H L, Nguyen H T, Bui S T, Le D T, Ngo Q M and Vu D L 2016 *Adv. Nat. Sci-Nanosci.* **7** 015015

[50] Tuong P, Yoo Y, Park J, Kim Y, Kim K, Kim Y, Cheong H, Chen L and Lee Y 2015 *Journal of Optics* **17** 125101

[51] Ordal M A, Bell R J, Alexander R W, Newquist L A and Querry M R 1988 *Appl. Opt.* **27** 1203